VESPA

PHYSICS DEGREE Academic Year 2021-2022

Group 17, cohort 3
Rachele Cicioni
Maria Sharon Di Spena
Giacomo Guastella

December 11, 2021

Abstract

The aim of the VESPA experiment is to form a plasma inside a discharge chamber, to perform a characterization of its behaviour through characteristic parameters.

Experimental SET-UP

The experimental set-up is composed by a vacuum system, allowing to get a low pressure gas volume, by an electric part, which allows forming the plasma and performing Langmuir probe measurements and by a system of permanent magnets, located at the inner side of the vacuum wall, which can improve plasma confinement and hence increase plasma density.
The scheme of the experimental apparatus (shown in **Figure 1**) is made of the following main components: a cylindrical vacuum chamber (length: 80 cm, diameter 40 cm) (3), divided into two halves by an electrostatically insulated grid; a turbomolecular pump (6), with dedicated power supply; a rotary pump (10) for the establishment of pre-vacuum condition necessary for the turbomolecular pump. A valve separating the chamber and the pumping system (5) is present; a needle valve and associated open/close valve(2) to fill the chamber with the gas. It is connected to the argon line (1); the throttle (butterfly valve) (8) for the turbomolecular pump ventilation;a pre-vacuum measurement gauge (Pirani) (7) and associated reading component. Also is present a vacuum measurement gauge (4)(ionization instrument, for vacuum measurement in the chamber) and associated reading component; an alumina trap (9), to absorb oil vapors from the rotary pump and at the end an exhaust pipe (11).

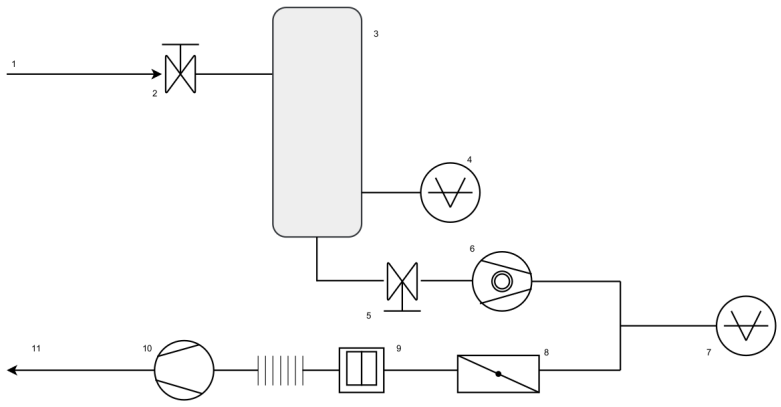

Figure 1: Experimental set-up.

In the inner side of the vacuum chamber, a system of permanent magnets improves plasma confinement and hence increase the plasma density.
In order to generate a plasma, it is necessary to apply an electric field to a neutral gas (for the VESPA experiment is been used Argon gas). The gas pressure has been lowered by the vacuum system to optimize the condition for the generation of the plasma. The application of an electric field accelerates the free electrons initially present in the gas. If the applied voltage is sufficiently strong, the collisions between them with the atoms of the gas will induce the gas ionization. The breakdown voltage is the voltage at which the avalanche process generates the plasma. In the VESPA experiment is possible to generate the plasma in two different ways as described in **section 3**: by thermionic emission of a heated tungsten filament (Length =10 cm and diameter 0.25 mm) that acts as cathode, while the chamber is the anode (DC condition), and then using a radiofrequency voltage (RF condition).
A Isotech power supply (output up to 36 V and 20 A) is used to drive the current in the filament in order to increase the temperature and so to increase emitted electron currents. Another Isotech power supply (output up to 100 V and 3 A) has been used for negative filament polarization with respect to the chamber electrically grounded. A 1 Ω resistor is mounted in series with the power supply to measure the plasma current by measuring the potential fall on the said resistor. A Kepco BOP 100-4M power supply (output up to ± 100 V and ± 4 A) is used to polarize the grid that divides into two parts the vacuum chamber. The apparatus is also composed of three system Langimur probes. Two of them are used to measure the plasma parameters and they are placed to the right and to the left of the grid. The other one is installed in the manipulator. The probes are made of tungsten wires (1 mm diameter) covered by a quartz tube, but 1 cm long piece of tungsten wire is exposed to the plasma. The probes are electrically connected to the outer part of the chamber by coaxial cables. The voltage applied to the probes is supplied by a power supply Kepco BOP 100-1M (output up to ± 100 V and ± 1 A).

1 Characterization of the vacuum system

The first operation performed in the laboratory is the study of the vacuum system. To characterize the pumping system the quantities studied are the limit pressure value, the pumping speed and the conductance.
In the beginning is performed a measure of the degassing of the system. In the first step the gas pressure is lowered in order to reach values around $p = 2.6 \times 10^{-5}$ mbar. Subsequently the valve connecting the vacuum chamber with the pumping system is closed. A rise in the pressure is expected due to leaks like small holes, evaporation of substances and other phenomena. If it is assumed that the pumping speed does not depend on the pressure, the theoretical expectation is a linear trend that follows the equation:

$$p(t) = p_0 + \frac{F_0}{V}t$$

where p_0 is the limit pressure, F_0 is the flow rate of the gas sources and V is the volume of the chamber. The error in the pressure measurement is obtained by the sensibility of the instrument due to a high fluctuation during the lecture of the measure. A second error is introduced by the time measurement in that it is to take into account both the reaction time of the operator and the time to pass from the chronometer to the instrument. For these reasons an error of 1 second is considered.
The data obtained shows non linear trend during the whole acquisition, as can be seen in the first graph of **Figure 2**. This is due to the fact the assumptions made before are not correct. In order to describe this variation from the theoretical linear expectation, is performed a linear fit in the first zone ([0-150] seconds range, Green line of equation $y = mx + q$), and then, at higher value of pressure, it is add a sinusoidal term ([150-600] seconds range, red line of equation $y = mx + q + Asin(kx)$). As it is shows in the second graph of **Figure 2**, is obtained a better match with the experimental points. So to compute the characteristic parameters of the chamber it is considered the first linear fit compared with the linear term of the second fit. The results of the fits are shown in **Table 1**.

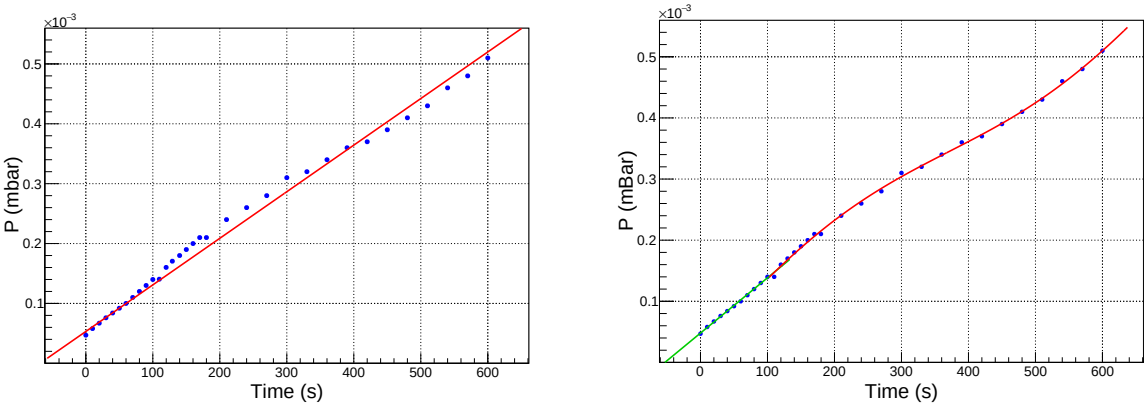

Figure 2: Pressure of degassing as a function of time: in the first graph is present a linear fit over the whole range according to the theoretical trend, in the second are presents both a linear fit in the first zone and a non linear fit in the rest in order to better describe the experimental trend.

m (mBar)	q (mBar/s)	χ^2/ndf
$(4.81 \pm 0.06) \cdot 10^{-5}$	$(9.0 \pm 0.1) \cdot 10^{-7}$	1.2

Table 1: Fit parameters of the pressure of degassing in function of time with a linear function in the range of [0-150] seconds (green line).

m (mBar)	q (mBar/s)	A (mBar/s)	k (1/s)	χ^2/ndf
$(2.2 \pm 0.6) \cdot 10^{-5}$	$(8.7 \pm 0.2) \cdot 10^{-7}$	$(3.7 \pm 0.3) \cdot 10^{-5}$	$(8.5 \pm 0.1) \cdot 10^{-3}$	1.4

Table 2: Fit parameters of the pressure of degassing in function of time with a linear function in the range of [150-600] seconds (red line).

As can be seen by the results of the χ^2, the two fits represent a good approximation of the trend (the linear fit over the total points returns a reducted $\chi^2 = 23$).
In a second moment, the valve that connects the chamber with the pumps is opened. A rapid lowering of the pressure in the chamber is expected. The trend follows by experimental data should follow an exponential function:

$$p(t) = (p_i - p_0)e^{-\frac{t}{\tau}} + p_0$$

where p_i is the initial pressure of the chamber. As can be seen in **Figure 3**, the trend is clearly exponential, however the fit is not optimal. This may be due to the fact that in the first zone of rapid decreasing, the values of the pressure has been taken at the complete opening of the valve. In that short period of time however the pressure decreased rapidly and for which not enough point were taken. The results of the fit are shown in **Table 3**.

p_0 (mBar)	τ (s)
$(4.89 \pm 0.06) \cdot 10^{-5}$	(41.7 ± 0.3)

Table 3: Fit parameters of the pressure in function of time with an exponential function.

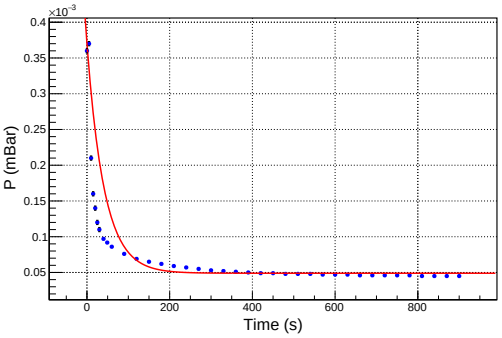

Figure 3: Pressure of pumping in function of time.

It is possible now to confront the characteristic parameters obtained by the two fits and to compute the conductivity of the connection between the chamber and the vacuum pumping system.

$$\frac{F_0}{V} = \frac{p_0}{\tau} = (1.17 \pm 0.02) \cdot 10^{-6} \ \frac{mBar}{s} \qquad S_e = \frac{V}{\tau} = 2.41 \pm 0.02 \ \frac{l}{s}$$

Knowing that the nominal pumping speed is $S = 33\ l/s$, the conductivity is:

$$C = \frac{S_e \cdot S}{S - S_e} = 2.60 \pm 0.02 \quad \frac{l}{s}$$

At the end, it is possible to compare the parameter F_0 obtained from the fit of the previous parts.

$$F_0^{lin} = (4.84 \pm 0.02) \cdot 10^{-8} \ \frac{mbar\ m^3}{s} \qquad F_0^{sin} = (2.2 \pm 0.6) \cdot 10^{-8} \ \frac{mbar\ m^3}{s} \qquad F_0^{exp} = (1.2 \pm 0.2) \cdot 10^{-7} \ \frac{mbar\ m^3}{s}$$

As it can be seen, the three values obtained by the different fits are not compatible. This is probably due to the fact that the exponential fit is not optimal, and the other two values are however in the same order of magnitude.

2 Voltage-Current characteristics of the filament

It is important to study the characteristics of the filament voltage-current curve. In the experiment it is considered a filament, where a current I_F is driven by a potential difference V_F applied to its extremals. The relation between I_F and V_F is given, following Ohm's law, by the filament resistance, that however depend on the temperature. It is possible to obtain a difference dependence through a second equation which comes from the balance between the Ohmic input power heating the filament and the radiated power from the filament itself. In this way, the theoretical laws are:

$$V_F = \rho(T) \frac{L}{\pi r^2} I_F \qquad V_F I_F = \epsilon \alpha T^4 2\pi r L \qquad \rho(T) = 6.2 \times 10^{-11} T^{1.2}$$

where α is the Boltzmann constant and ϵ is the effective emissivity of the filament. It is therefore possible to obtain a formula for the voltage as function of the current:

$$V_F = \left[\frac{6.2 \times 10^{-11} L}{\pi r^2 (\epsilon \alpha 2\pi r L)^{0.3}} \right]^{\frac{10}{7}} I_F^{\frac{13}{7}}$$

As is seen in **Figure 4**, the data does not follow the theoretical expectation (green line). This is probably due to the fact that the emissivity of the tungsten can change because of an excessive wear of the filament. So, it is performed a fit of the voltage - current trend, with ϵ as parameter, to compare with the expected value of 0.3. At the end, it is shown the graph of the estimated filament temperature as a function of the driven current.

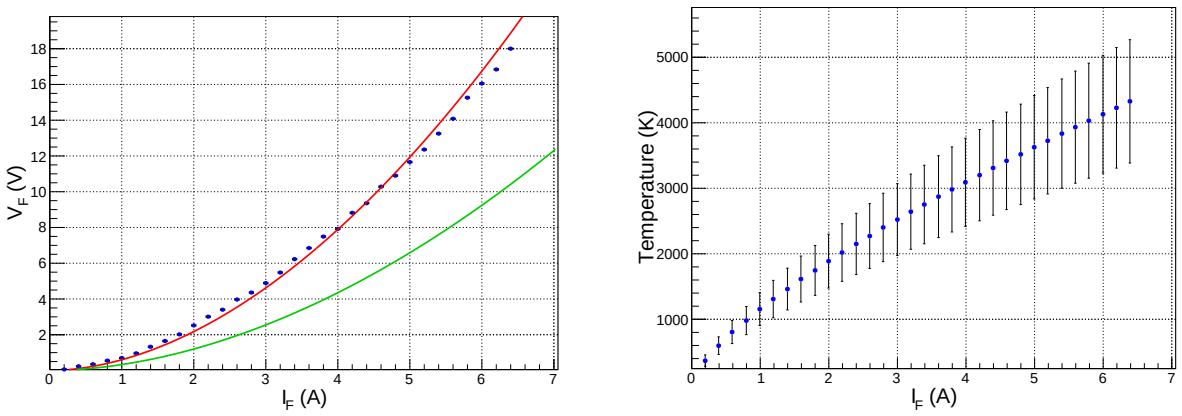

Figure 4: 1^{st} graph: the characteristics voltage-current curve of the filament: in green the theoretical expectation ($\epsilon = 3$), in red the fit. 2^{nd} graph: filament temperature as a function of the driven current.

Parameter	Fit Result
ϵ	0.08 ± 0.04

Table 4: Values obtained for the fit $V_F = \gamma \epsilon^{-3/7} I_F^{13/7}$

The first graph in **Figure 4** and the result from **Table 4**, shows that the filament has a very different emissivity from the expected value. As said before this is due to the excessive wear of the filament. In fact the wire has been already use for the same experiment the previous week, and this may be the reason for its consumption.

3 Breakdown curves and Paschen curves in DC and RF condition

After studying the characteristics of the filament, tungsten is used as a hot cathode: by inducing a current in the tungsten filament and exploiting the phenomenon of thermionic emission of electrons for its part, the emitted electrons are accelerated by means of an electric field, in order to induce an ionization of the Argon gas present in the vacuum chamber, and therefore the onset of the plasma. This onset occurs for a certain voltage value across the two electrodes, called *breakdown voltage*. This voltage, and therefore the onset of the plasma itself, depends on the current induced in the tungsten filament and on the pressure of the Argon gas. The study of the dependence of the breakdown curves on these physical quantities is therefore relevant. In particular, if a cold cathode is used, the breakdown voltage is a function of the product of the gas pressure and the distance between the electrodes:

$$V_b = \frac{BPd}{log(Apd) - log(log(1 + \frac{1}{\gamma}))}$$

where A, B, and γ are coefficients that depend on the type of gas and on the material of the electrodes. The curves described by this function are called *Paschen curves*. This curve present a minimum that in terms of the product $P \cdot d$ represents the best condition for plasma production. If a hot cathode is used, Paschen's theory doesn't hold anymore, but the trend of the breakdown voltage remains the same shape, with a dependence on the product $P \cdot d$ and a minimum which indicates ideal conditions. To observe the characteristics of the plasma it is therefore interesting to study the trend of the breakdown potential as a function of the gas pressure. This is done using two different methods to polarize the chamber: by using a constant electric field (DC condition), and by using an oscillating one (RF condition).

Breakdown curves for different values of filament current

To understand how the filament current influences the creation of the plasma, breakdown curves are constructed, keeping fixed the value of the pressure at $P = 2 \cdot 10^{-3} mbar$, and slowly increasing the voltage applied between the filament and the chamber, collecting the corresponding values of the plasma current. The procedure is repeated for three different values of the filament current. These values were chosen on the basis of the characteristics of the filament and of the generator used to polarize the camera. Indeed, probably due to the fact that the length of the filament has been varied and its reduced efficiency, attempts to generate the plasma for current values lower than $I_F = 5.9A$ didn't produce results, while it was not possible to rise above values equal to $I_F = 6.4A$ due to a generator saturation limit. The errors on current and voltage were considered as sensibility of the reading instrument, due to the high fluctuations in the values recorded by the instruments during the acquisition, while the error on the pressure takes into account the fact that it has been difficult to keep it constant. This implies an overestimation of the errors on the data, but in this way is taken into account the very high fluctuations from which they are affected. The trend of the breakdown curves, i.e. of the plasma current as a function of the applied voltage, for different values of I_F is shown in the **Figure 5**.

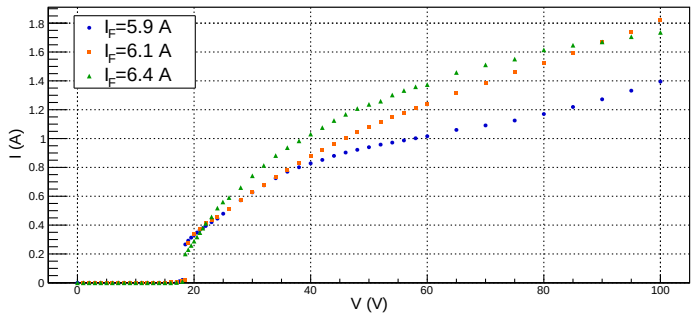

Figure 5: Breakdown curves for different values of the current filament I_F at fixed pressure of the gas $P = 2 \cdot 10^{-3} mbar$

I_F (A)	V_b (V)	P (mbar)	I (A)
5.9 ± 0.1	18.5 ± 0.1	$(2.0 \pm 0.5) \cdot 10^{-3}$	0.266 ± 0.001
6.1 ± 0.1	19.0 ± 0.1	$(2.0 \pm 0.5) \cdot 10^{-3}$	0.276 ± 0.001
6.4 ± 0.1	18.5 ± 0.1	$(2.0 \pm 0.5) \cdot 10^{-3}$	0.200 ± 0.001

Table 5: Values of plasma current and breakdown voltage for different values of filament current and fixed value of pressure.

From the theory it is expected that the breakdown voltage does not depend on the filament current, but only on the gas pressure, while once the plasma is ignited, the plasma current grows more rapidly as the voltage increases for higher values of I_F. Indeed, higher currents in the filament correspond to higher energy of the electrons produced by the thermionic effect, therefore higher levels of ionization. From the graph in the **Figure 5** and the values shown in the **Table 5** it can be seen that the value of V_b is approximately constant for all values of I_F, even if for $I_F = 6.1A$ a slight fluctuation is present. The plasma current of the filament also exhibits an abnormal behavior for $I_F = 6.4A$, being lower than the previous values. These slight discrepancies are not of concern, however, and are probably due to fluctuations of the gas pressure, which tended to decrease during measurements due to a momentary failure in the experimental setup, and of the filament current, which also decrease during the acquisition of the experimental data, likely due to the too high temperature of the cathode for higher values of I_F, so that is difficult for the generator to keep the current constant.

Breakdown curves for different values of gas pressure

By keeping the filament current fixed at the value $I_F = 6.1A$, the behavior of the breakdown curves for different values of the Argon pressure is also analyzed, and it is shown in the **Figure 6**. As in the previous section, errors are considered as instrument sensibility, for the same reasons.

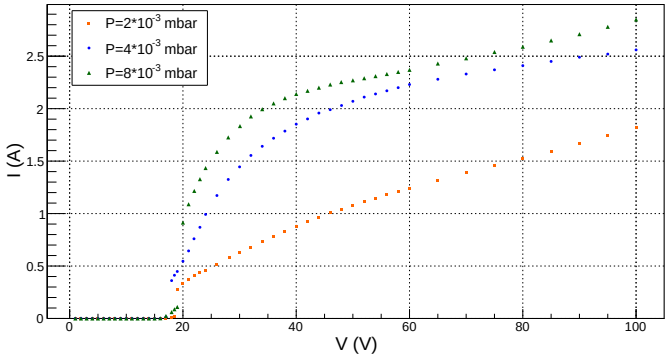

Figure 6: Breakdown curves for different values of the Argon pressure P at fixed filament current $I_F = 6.1A$

I_F (A)	V_b (V)	P (mbar)	I (A)
6.1 ± 0.1	19.0 ± 0.1	$(2.0 \pm 0.5) \cdot 10^{-3}$	0.276 ± 0.001
6.1 ± 0.1	18.0 ± 0.1	$(4.0 \pm 0.5) \cdot 10^{-3}$	0.361 ± 0.001
6.1 ± 0.1	20.0 ± 0.1	$(8.0 \pm 0.5) \cdot 10^{-3}$	0.914 ± 0.001

Table 6: Values of plasma current and breakdown voltage for different values of Argon pressure and fixed value of filament current.

Note that, also in this case, the pressure of the gas and the filament current tend to decrease during the acquisition of the experimental data, again due to a failure of the experimental setup. Nevertheless, as expected from the theory, the breakdown voltage depends on the pressure of the gas, while once this point has been passed the plasma current grows more for higher pressure values. Indeed, for higher pressures of the gas the free mean path for the electrons is smaller, so that the probability to ionize an atom is higher.

Paschen curve in DC condition

In order to build the Paschen curve in DC condition, the filament current is kept fixed at the value $I_F = 6.1A$ and values of breakdown voltage corresponding to different values of Argon pressure are collected. The obtained Paschen curve is shown in the **Figure 7**. Errors on the gas pressure and on the breakdown voltage are taken as the sensibility of the instruments.

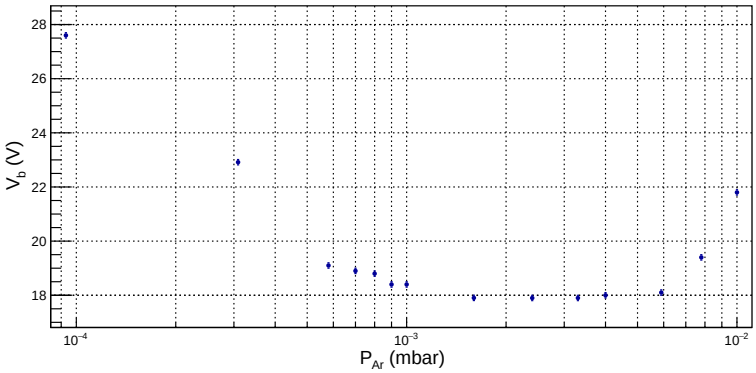

Figure 7: Paschen curve in DC condition for filament current value $I_F = 6.1A$: breakdown voltage V_b as function of the gas pressure P.

The shape of the curve obtained is exactly what was expected, with a minimum of the breakdown voltage and an increase of it for values of pressure too high or too low. The value of pressure corresponding to the minimum value of V_b is obtained taking the average between the three point which are at the same minimum level:

$$P_{min}^{DC} = (2.43 \pm 0.01) \cdot 10^{-3} mbar \qquad V_{b_{min}}^{DC} = (17.9 \pm 0.1) V$$

Paschen curve in RF condition

In this part of the experiment plasma is produced using no more the tungsten filament as hot cathode and a constant electric field in order to polarize the chamber, but by using a single electrode formed of permanent magnets polarized by an oscillating electromagnetic field, i.e. by a radiofrequency voltage. An inductance is used in order to amplify the applied voltage. The RLC circuit is then studied in order to work at the resonance frequency, and so to get the maximum signal amplification. Once obtained the resonance curve of the circuit, the value of the resonance frequency is used in order to build the Paschen curve in this condition: by varying the peak-peak voltage applied to the magnetized electrode,

the breakdown voltage is individuated, and so its dependence on the Argon pressure is collected. The Paschen curve obtained is shown in the **Figure 8**.

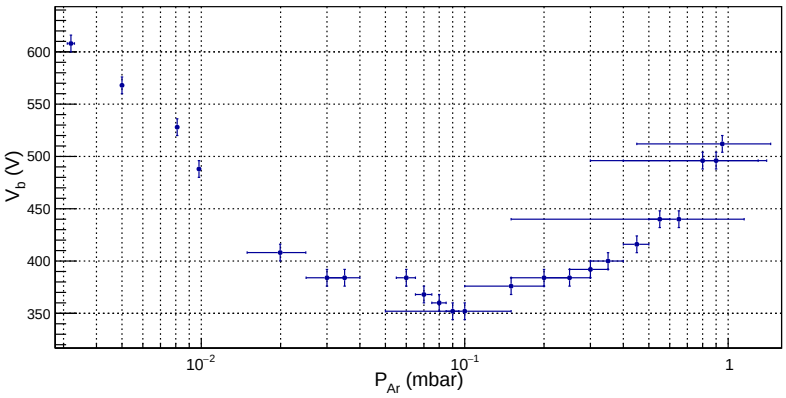

Figure 8: Paschen curve in RF condition: breakdown voltage V_b as function of the gas pressure P.

Also in this case the shape of the curve is consistent with the theoretical expectations: the breakdown voltage has a minimum for the pressure value

$$P_{min}^{RF} = (1.0 \pm 0.5) \cdot 10^{-1} mbar \qquad V_{b_{min}}^{RF} = (352 \pm 8) V$$

In the case of RF condition the optimal value of pressure in order to produce a plasma and the value of the breakdown voltage are much higher than in the case of DC condition. This was expected and it is due to the fact that the length that electrons feels is no more the distance between the cathode and the anode, but it is the length related to the oscillating electric field, which is much smaller.

4 Measurements of plasma parameters

With the Langmuir probes it's possible to obtain the characteristic quantities of the electrons. The Langmuir probes are diagnostic electrodes inserted inside the plasma, whose characteristic curve I(V), shown in **Figure 9**, has the following analytical expression:

$$I = I_s \left[exp\left(\frac{e(V - V_f)}{kT_e} \right) - 1 \right]$$

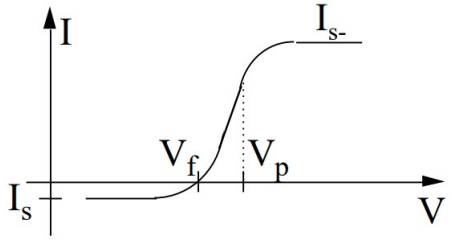

Figure 9: Electrical voltage-current characteristics of a Langmuir probe.

where V_f is the floating potential, i.e. the potential reached spontaneously by an object inserted in the plasma, T_e is the electrons temperature, k the Boltzmann constant and I_s is the ion saturation current give by the expression:

$$I_s = \frac{1}{2} A e n c_s$$

where A is the Langmuir probe area, n the density and c_s the so-called *ion sound velocity*, i.e. the sound velocity of a system made of ions. For the floating potential we have the following equation:

$$Vf = V_p + \alpha k T_e / e$$

where V_p is the plasma potential and $\alpha = \frac{1}{2}log(\frac{\pi m}{2M})$ is a constant and for the Argon it's -5.4.
The Argon valve was slowly opened to reach a pressure at the value of 2.2×10^{-3} mbar, close to the minimum value found in the experimental Paschen curve of the previous point. The filament current was slowly brought to 6.1A. A preliminary measurement was made and it was seen that by varying the discharge polarization voltage from 20V to 80V, the filament current did not remain stable. At the value of 80V the current dropped down to the value of 5.8A and for this value the filament current remained stable in the voltage range required. For this reason the filament current has been fixed at 5.8A. Setting the different discharge polarization voltages, the I(V) characteristic curve of the Langmuir probes was obtained using the LabView software.
For each discharge polarization voltage value, two curves were taken: the curve of the the probes near the filament (to the *right* of the grid) and the curve of the probes far from the filament (to the *left* of the grid). The fit of the curves was done by using the appropriate software and by choosing the curve data up to the exponential growth preceding the electronic saturation current. The values collected for each fit are T_e, V_p and n. All values are recorded in **Table 7** and for each values it was estimated an absolute error of 10% visible in the graphs. In **Figure 10, 11, 12** the trends of these parameters are shown as a function of the plasma current I_{dis}.

V_{dis}(V)	T_e(eV)		n(m^{-3})		V_p(V)		I_{dis}(A)
	right	*left*	*right*	*left*	*right*	*left*	
20.5	0.9764	0.6574	$1.07{\cdot}10^{16}$	$6.99{\cdot}10^{15}$	1.93	1.57	0.429
30.5	0.9006	0.6841	$3.36{\cdot}10^{16}$	$9.80{\cdot}10^{15}$	2.21	1.38	0.858
40.5	1.2880	0.7269	$5.28{\cdot}10^{16}$	$1.63{\cdot}10^{16}$	3.28	1.58	1.18
50.5	0.9770	0.7829	$7.81{\cdot}10^{16}$	$2.50{\cdot}10^{16}$	2.57	2.32	1.47
60.5	1.0215	0.8160	$1.07{\cdot}10^{17}$	$2.59{\cdot}10^{16}$	3.11	1.88	1.78
80.5	1.1785	0.9139	$1.94{\cdot}10^{17}$	$3.84{\cdot}10^{16}$	4.32	2.06	2.22

Table 7: Values of T_e, n and V_p obtained for each discharge plasma voltage and for each position of the probes with the software Labview.

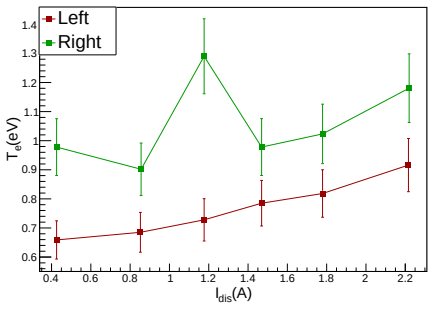

Figure 10: T_e as a function of I_{dis}.

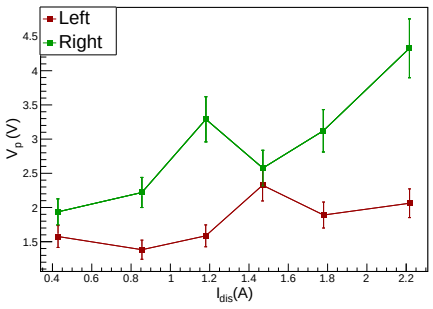

Figure 11: V_p as a function of I_{dis}.

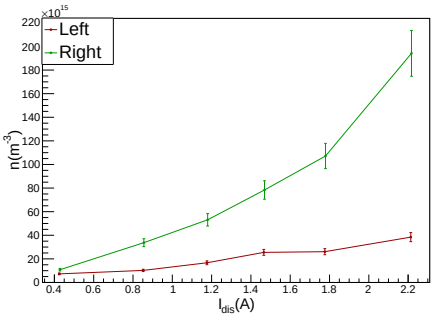

Figure 12: n as a function of I_{dis}.

For each density value n it's possible to calculate the ionization fraction f given by the following formula:

$$f = \frac{n}{n + n_0}$$

where n_0 is the neutral atom gas density. To evaluate n_0, the ideal gas law is used considering the environment at a temperature of 293K:

$$n_0 = \frac{p}{kT}$$

The **Table 8** shows the ionization fractions obtained.

V_{dis}	p(mbar)	$n_0(m^{-3})$	*f left*	*f right*
20.5	$(2.3\pm0.1)\cdot10^{-3}$	$(5.686\pm0.002)\cdot10^{19}$	$(1.2\pm0.1)\cdot10^{-4}$	$(1.8\pm0.2)\cdot10^{-4}$
30.5	$(2.3\pm0.1)\cdot10^{-3}$	$(5.686\pm0.002)\cdot10^{19}$	$(1.7\pm0.2)\cdot10^{-4}$	$(5.9\pm0.6)\cdot10^{-4}$
40.5	$(2.2\pm0.1)\cdot10^{-3}$	$(5.438\pm0.002)\cdot10^{19}$	$(3.0\pm0.3)\cdot10^{-4}$	$(1.0\pm0.1)\cdot10^{-3}$
50.5	$(2.1\pm0.1)\cdot10^{-3}$	$(5.191\pm0.002)\cdot10^{19}$	$(4.8\pm0.5)\cdot10^{-4}$	$(1.5\pm0.2)\cdot10^{-3}$
60.5	$(2.2\pm0.1)\cdot10^{-3}$	$(5.438\pm0.002)\cdot10^{19}$	$(4.8\pm0.5)\cdot10^{-4}$	$(2.0\pm0.2)\cdot10^{-3}$
80.5	$(2.2\pm0.1)\cdot10^{-3}$	$(5.438\pm0.002)\cdot10^{19}$	$(7.1\pm0.7)\cdot10^{-4}$	$(3.6\pm0.4)\cdot10^{-3}$

Table 8: The constant fraction obtained for each value of n.

5 Ion acoustic wave propagation

In the plasma it is possible to have the so-called ion acoustic waves. They are perturbations that do not propagate through binary collisions between particles but thanks to the oscillations of ions and electrons present in the plasma. The dispersion relationship of ion acoustic waves is:

$$\frac{w}{k} = c_s$$

Where c_s is given by law:

$$c_s = \sqrt{\frac{kT_e}{m_i}}$$

where m_i is the mass of ions. In the vacuum chamber it is possible to induce an ion acoustic wave by polarizing the grid with an oscillating voltage at a frequency of 20 kHz. This perturbation propagates in the plasma but, due to the interactions of ions and electrons with neutral particles, part of the energy is lost and the wave is damped. The amplitude of the ion acoustic wave therefore follows an exponential decay law where δ is the decay length:

$$V(x) = V_0 e^{-\frac{x}{\delta}} \qquad \delta = \frac{2c_s}{\nu_{e0}}$$

The term ν_{e0} is the collision frequency between electrons and neutral particles:

$$\nu_{e0} = v_{te} n_0 \sigma_0 = \sqrt{\frac{8kT_e}{\pi m}} n_0 \sigma_0$$

The pressure in the chamber was brought to 5.1×10^{-4} mbar. Preliminary measurements were made about the discharge polarization voltage to be set to study the decay law of the wave amplitude. This was set at 40V and 70V and the wave amplitude and phase shift measurements were taken for each of them. From this preliminary analysis it was decided to set the voltage at 40V since the data followed a more pronounced exponential trend. Subsequently, using the appropriate manipulator, the Langmuir probes were moved, which collected the density fluctuation. For different distances were taken the phase difference values between the fluctuations detected by the Langmuir probes and the voltage induced to the grid, and peak-to-peak amplitude. The values obtained are in **Table 9**. For the error on the amplitude Pk-Pk, it was considered an error of 10% due to the fluctuation of the values at the time of the measurement.

From the values of x and Δt it's possible to obtain the experimental value of c_s. From the linear fit of the data, in **Figure 13**, we obtained an angular coefficient $m = (-1.65 \pm 0.02)^{-2}$ cm/μs from which we can obtain the experimental value of $c_s = (165 \pm 2) \times 10$ m/s.
To make a comparison with the previous point, the values of c_s are calculated for the temperatures T_e obtained with the use of Langmuir probes using the analytical expression for c_s. The T_e *left* values were considered since Langmuir probes far from the filament were also used in this part of the experience. The **Table 10** shows the temperatures T_e and the respective values of c_s. The graph in **Figure 14** shows the values of the table obtained from the theoretical expression (the trend $c_s(T_e)$ is represented by the dashed curve) and in green is the value c_s obtained from the sound ion waves by estimating

x (cm)	$\Delta t(\mu s)$	Pk-Pk (V)
34.5±0.1	2.6±0.2	1.7002
34.0±0.1	5.1±0.2	1.6050
33.5±0.1	7.9±0.2	1.6055
33.0±0.1	10.8±0.2	1.5910
32.5±0.1	12.7±0.2	1.4553
32.0±0.1	15.8±0.2	1.3160
31.5±0.1	18.2±0.2	1.1905
31.0±0.1	21.2±0.2	1.0104
30.5±0.1	24.3±0.2	0.8712
30.0±0.1	27.5±0.2	0.7235
29.5±0.1	30.9±0.2	0.6625
29.0±0.1	35.2±0.2	0.6059
28.5±0.1	37.3±0.2	0.5837
28.0±0.1	40.3±0.2	0.5200
27.5±0.1	43.5±0.2	0.5253
27.0±0.1	48.0±0.2	0.5214
26.5±0.1	50.3±0.2	0.5502

Table 9: Values of the ion acoustic wave for different distances.

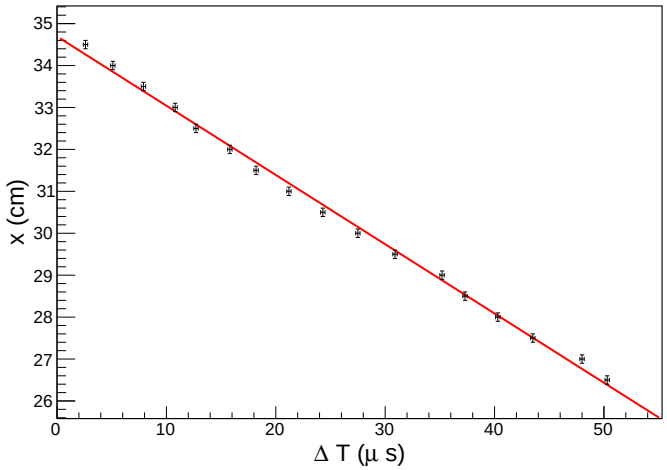

Figure 13: The linear fit to evaluate c_s.

a temperature T_e about 1eV. The latter differs from the theoretical curve but this may be due to an imprecision in the estimate of T_e which is probably greater than 1eV. In general, however, we can affirm that the values of c_s obtained with Langmuir probes and with sound ionic waves are of the same order of magnitude.

The **Figure 15** shows the exponential fit of the amplitude damping as a function of the position

$T_e(K)$	$c_s(m/s)$
7629	$(126\pm6)\cdot10^1$
7939	$(129\pm6)\cdot10^1$
8435	$(133\pm7)\cdot10^1$
9085	$(138\pm7)\cdot10^1$
9469	$(140\pm7)\cdot10^1$
10605	$(149\pm7)\cdot10^1$

Table 10: Values of c_s calculated with T_e *left* of the Langmuir probes.

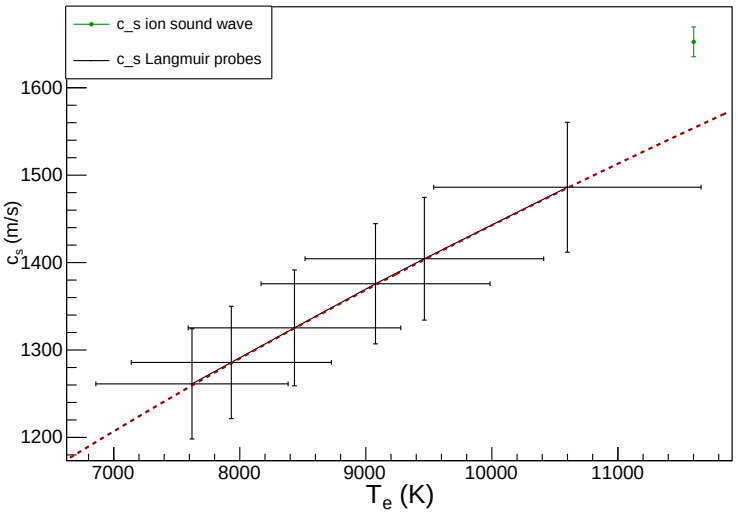

Figure 14: Comparison between c_s of the ion sound wave and c_s of the Langmuir probes.

of the Langmuir probes. It was decided to neglect the data that differed most from the exponential trend. The δ value of the decay law obtained from the fit is:

$$\delta = (4.2 \pm 0.4)cm$$

With this δ value it is possible to calculate the value of n_0 considering a temperature T_e of 1 eV and

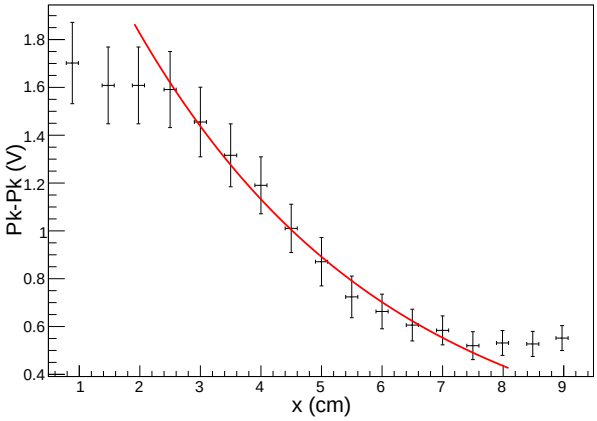

Figure 15: Exponential fit for the decay law for the amplitude.

compare it with the value obtained from the ideal gas law:

$$n_{0\,fit} = (5.9 \pm 0.5) \cdot 10^{18} m^{-3} \qquad n_{0ideal} = (1.26 \pm 0.03) \cdot 10^{19} m^{-3}$$

The discrepancy obtained between the values of n_0 is probably due to the data collected to obtain the decay law, which did not follow an exponential trend as expected.

Conclusion

In the Vespa experiment has been studied the vacuum system through characteristic parameters: limit pressure value, the pumping speed and the conductance. Subsequently was studied the voltage-current characteristic of the filament through which is obtained the effective values of the emissivity of the filament ($\epsilon \sim 0.08$). It is then plotted the Breakdown and Paschen curves in DC and RF condition in order to verify the pressure dependence of the breakdown voltage, and also the dependence on the current filament. It is then confirmed that in RF condition it is possible to generate the Plasma at higher pressure due to the smaller distance between electrodes felt by the electrons. The value of the ion sound velocity obtained with the characterization of the ion acoustic waves is of the same order of magnitude as that obtained with the Langmuir probes. On the other hand, from the fit for the decay law of the wave amplitude as a function of distance, a value of n_0 was obtained slightly in disagreement with the theoretical one.